ELSEVIER

Fluid Phase Equilibria 187–188 (2001) 71–82

FLUID PHASE EQUILIBRIA

www.elsevier.com/locate/fluid

Measurement and prediction of temperature and pressure effect on wax content in a partially frozen paraffinic system

Jérôme Pauly [a], Jean-Luc Daridon [a,*], João A.P. Coutinho [b]

[a] *Laboratoire des Fluides Complexes, Groupe Haute Pression, Université de Pau, BP 1155, 64013 Pau Cedex, France*
[b] *Departamento de Química da Universidade de Aveiro, 3810 Aveiro, Portugal*

Received 16 January 2001; accepted 8 May 2001

Abstract

Liquid–solid phase equilibrium measurements were carried out at various pressures and temperatures below the onset of crystallization in a mixture made up of a distribution of paraffins with composition exponentially decreasing from *n*-C_6 to *n*-C_{36}. Liquid and solid phases in partially frozen mixtures were separated by isobaric and isothermal filtration and analyzed by gas chromatography. Waxy solid content and wax composition were then deduced from a mass balance after correction for the entrapped liquid in the solid residue. The results were then compared to the prediction of a model which was previously developed for the representation of the wax appearance temperature of synthetic light gas–heavy paraffins systems.

Keywords: Solid–liquid equilibrium; Pressure; Wax; Paraffin

1. Introduction

Most petroleum reservoir fluids contain heavy hydrocarbons which may precipitate as a waxy solid phase when conditions of temperature and pressure change. As the wax formation appears in cool environment, most of the experimental work on the formation of waxes has been restricted to the measurement of wax appearance temperature or to the study of the effect of temperature on the amount and the composition of solid deposits at atmospheric pressure. However, although it is less significant, the influence of pressure on the wax content in partially paraffinic systems is not negligible.

In order to quantify the effect of pressure as well as temperature on the formation of waxy deposits, the amount and the composition of wax were measured in a partially frozen mixture made up of a distribution of paraffins with concentration regularly decreasing from C_6 to C_{36} representing a highly simplified model of a crude oil. Measurements were performed up to 50 MPa by phase separation in a filtration cell and analyzed, by GC chromatography, of both filtrate and residue of filtration.

* Corresponding author. Tel.: +33-55992-3337; fax: +33-55980-8382.
E-mail address: jean-luc.daridon@univ-pau.fr (J.-L. Daridon).

0378-3812/01/$ – see front matter
PII: S0378-3812(01)00527-1

The experimental data were then compared with those predicted by a model developed previously [1] for predicting the wax appearance temperature at high pressure conditions. Two different approaches for the description of the non-ideality of the solid solutions were tested.

2. Experimental technique

In a homogenous liquid made up of one or more solvents and of a series of heavy paraffins between C_{18} and C_{50} such as heavy oils, fuels or synthetic systems, changes of pressure or reduction of temperature can cause precipitation of some of the paraffins in the form of wax. To characterize the quantity and composition of waxes as a function of pressure we have used an isobaric filtration method which can isolate a part of the liquid phase from the rest of the system [2]. The filtration cell (Fig. 1) comprises two stainless steel autoclave cylinders (1) and (6) separated by a filtration system (2) (a disc of sintered steel of 3 μm porosity, 20 mm in diameter and 1 mm thick) and closed at their extremities by pistons (5) which separate the sample studied and the compression oil. In order to be able to recover both the filtration residue and the sintered steel disc easily, the chamber (1) which holds the initial fluid can be entirely dismantled. The second chamber which has to take the liquid filtrate is machined directly in the body of the cell. To ensure satisfactory thermal uniformity within the fluid, the cell is fully immersed in a refrigerated thermostat bath (Huber) which is agitated and thermo-regulated by a Bioblock thermostat with a stability of 0.02 K. The temperature was measured by means of a platinum probe placed inside the cylinder containing the initial fluid and linked to an AOIP brand thermometer. Pressure is measured by means of two HBM manometers equipped with P3M probes placed in the compression oil circuit ensuring a measurement accuracy within the sample of 0.05 MPa after correction for the pressure drop generated by friction of the pistons in the cell.

The mixture is first prepared by weighing in a reservoir bottle and then introduced in monophasic state into the cylinder of the filtration cell, where it is brought to the required pressure and temperature conditions. It is kept in this state for 24 h in order to ensure that the system is kinetically stable and in thermodynamic equilibrium.

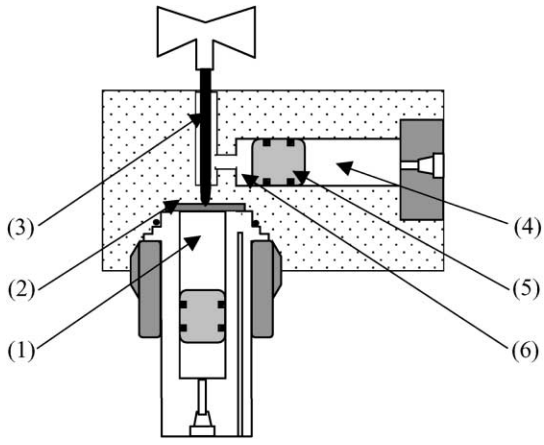

Fig. 1. Filtration cell: (1) equilibrium system cylinder; (2) filtration disc; (3) separation valve; (4) compression oil; (5) piston; (6) filtrate cylinder.

The two bodies of a double body volumetric pump are then activated synchronously, but in phase opposition to displace the fluid under pressure through the sintered steel disc. The liquid filtrate and the solid residue as well as the sintered metal discs are then recovered, weighed and analyzed by gas chromatography.

The analysis of the filtrate directly gives the composition of the liquid phase. However, a large proportion (up to 40% of the solid residue) of liquid remains trapped with the waxes in the solid residue, and thus, the amount of solid residue do not correspond to the amount of solid in the system in equilibrium. To assess the real wax content and compositions, it is necessary to determine the quantities of liquid trapped. The selected method, which rests solely on compositional analysis (in mass fraction) of the filtrate w_i^{L} and knowledge of the overall composition z_i (in mass fraction) of the system studied, consists of determining the real mass fraction of liquid, L in the muti-phase system using the fact that the components of the solvent (the lightest alkane) does not precipitate:

$$\mathrm{L} = \frac{z_{\mathrm{solvent}}}{w_{\mathrm{sovent}}^{\mathrm{L}}} \tag{1}$$

It is thus, possible to calculate the quantity and composition of the solid deposit using the mass balance:

$$\mathrm{S} = 1 - \mathrm{L} \tag{2}$$

$$w_i^{\mathrm{S}} = \frac{z_i - \mathrm{L}\, w_i^{\mathrm{L}}}{1 - \mathrm{L}} \tag{3}$$

With the aim to study the influence of pressure an temperature on partially frozen systems, a series of measurements was made on a synthetic mixture. Measurements were carried out on a system composed of the full series of *n*-paraffins within which the mole fraction Z_i of *n*-paraffins is regularly decreasing from C_6 to C_{36} according to the recurrence relationship:

$$Z_{\mathrm{C}_{n+1}} = \alpha Z_{\mathrm{C}_n} \tag{4}$$

where the coefficient α was fixed at 0.885 to match the average compositions observed in waxy crude oils. Table 1 presents the overall composition (mass%) of the system studied as well as their purities.

The experiments were carried out at 0.1, 10 MPa, 30 and 50 MPa and at selected temperatures below the wax appearance temperature. The results obtained for the waxy solid phase, after correction for the quantities of trapped liquid, are summarized in Table 2. From this table it can be seen that an increase in pressure produces effects similar to those caused by a decrease in temperature. To study the influence of both temperature and pressure in more detail, we calculated the percentage (in mass) of paraffin crystallized PC_i for each paraffin *i* which can be derived directly from the experimental data by

$$\mathrm{PC}_i = 100 \times \left[1 + \frac{\mathrm{L}w_i^{\mathrm{L}}}{\mathrm{S}w_i^{\mathrm{S}}}\right]^{-1} \tag{5}$$

The corresponding results are listed in Table 3 as a function of the carbon number. As an illustration, a few isotherms and isobars are plotted in Figs. 2 and 3, respectively. It can be observed that the isothermal curves which are quite regular in shape, are shifted towards the lighter paraffins when pressure increases. In the same way, the isobaric curves tend to move to the lower paraffins when temperature decrease. This identity, shows that an increase in pressure produces effects comparable to those caused by a reduction in temperature.

Table 1
Feed composition (wt.%) of the system

Components	wt.%	Reference	Purity	Components	wt.%	Reference	Purity
n-C_6	11.71	Aldrich	>99	n-C_{22}	1.34	Aldrich	>99
n-C_7	11.12	Aldrich	>99	n-C_{23}	1.12	Aldrich	>99
n-C_8	10.09	Aldrich	>99	n-C_{24}	0.94	Fluka	>99
n-C9	9.11	Aldrich	>99	n-C_{25}	0.79	Fluka	>98
n-C_{10}	8.13	Aldrich	>99	n-C_{26}	0.66	Aldrich	>99
n-C_{11}	7.08	Aldrich	>99	n-C_{27}	0.55	Fluka	>98
n-C_{12}	6.22	Aldrich	>99	n-C_{28}	0.46	Fluka	>98
n-C_{13}	5.39	Aldrich	>99	n-C_{29}	0.38	Fluka	>99.5
n-C_{14}	4.69	Aldrich	>99	n-C_{30}	0.31	Aldrich	>99
n-C_{15}	4.10	Aldrich	>99	n-C_{31}	0.26	Kasei	>97
n-C_{16}	3.54	Aldrich	>99	n-C_{32}	0.22	Kasei	>98
n-C_{17}	3.02	Aldrich	>99	n-C_{33}	0.18	Kasei	>95
n-C_{18}	2.57	Fluka	>99	n-C_{34}	0.15	Kasei	>98
n-C_{19}	2.21	Aldrich	>99	n-C_{35}	0.12	Kasei	>95
n-C_{20}	1.88	Aldrich	>99	n-C_{36}	0.10	Kasei	>95
n-C_{21}	1.58	Fluka	>98				

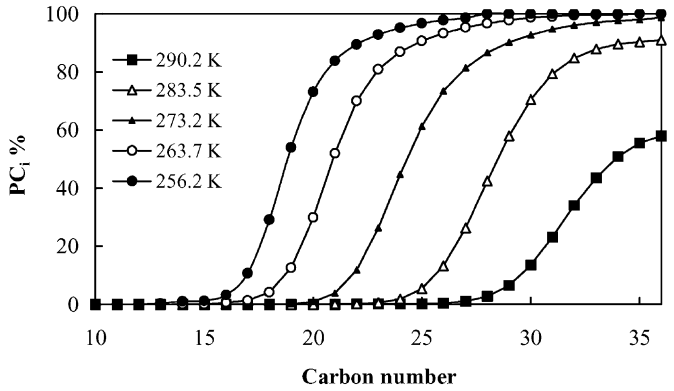

Fig. 2. Weight percentage of paraffins crystallized at various temperatures and at atmospheric pressure.

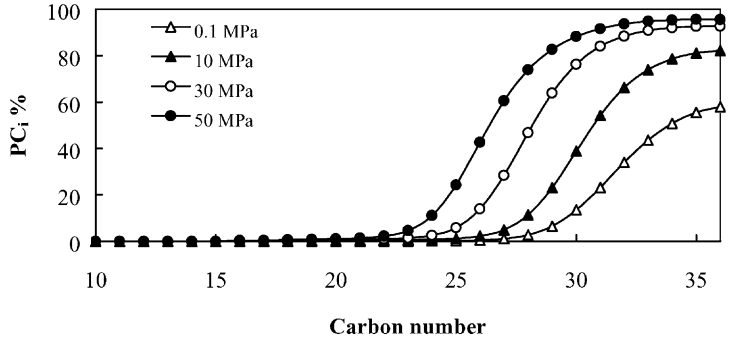

Fig. 3. Weight percentage of paraffins crystallized at various pressure and at 290.2 K.

Table 2
Quantity and composition of the solid deposit at the studied (P, T) conditions

P (MPa)			0.1				10			30			50
T (K)	290.2	283.5	273.2	263.7	256.2	290.2	273.2	256.2	290.2	273.2	256.2	290.2	273.2
Solid deposit (mass%)	0.46	1.38	4.57	9.40	14.81	1.42	5.97	17.35	2.78	7.46	18.14	4.83	9.36
Solid phase composition (mass%)													
C_6	0.00	0.00	0.00	0.00	0.00	0.00	0.00	0.00	0.00	0.00	0.00	0.00	0.00
C_7	0.00	0.00	0.00	0.00	0.00	0.00	0.00	0.00	0.00	0.00	0.00	0.00	0.00
C_8	0.00	0.00	0.00	0.00	0.00	0.00	0.00	0.00	0.00	0.00	0.00	0.00	0.00
C9	0.00	0.00	0.00	0.00	0.00	0.00	0.00	0.00	0.00	0.00	0.00	0.00	0.00
C_{10}	0.00	0.00	0.00	0.00	0.00	0.00	0.00	0.00	0.00	0.00	0.00	0.00	0.00
C_{11}	0.00	0.00	0.00	0.00	0.00	0.00	0.00	0.00	0.00	0.00	0.00	0.00	0.00
C_{12}	0.00	0.00	0.00	0.00	0.00	0.00	0.00	0.00	0.00	0.00	0.00	0.00	0.00
C_{13}	0.00	0.00	0.00	0.00	0.10	0.00	0.00	0.00	0.00	0.00	0.09	0.00	0.00
C_{14}	0.00	0.00	0.00	0.00	0.35	0.00	0.00	0.00	0.00	0.00	0.39	0.00	0.00
C_{15}	0.00	0.00	0.00	0.00	0.33	0.00	0.00	0.00	0.00	0.00	0.71	0.00	0.12
C_{16}	0.00	0.00	0.00	0.25	0.77	0.00	0.00	0.65	0.00	0.02	2.13	0.26	0.11
C_{17}	0.00	0.00	0.00	0.43	2.24	0.00	0.00	2.62	0.00	0.03	5.29	0.24	0.24
C_{18}	0.00	0.00	0.00	1.14	5.37	0.00	0.00	6.20	0.00	0.23	8.86	0.35	0.76
C_{19}	0.00	0.00	0.05	2.99	9.00	0.25	0.23	9.59	0.33	0.87	10.63	0.37	2.20
C_{20}	0.00	0.00	0.41	6.19	10.82	0.43	0.89	10.85	0.34	2.50	10.56	0.39	5.03
C_{21}	0.09	0.07	1.37	9.34	10.70	0.51	2.47	10.50	0.35	5.41	9.65	0.42	8.35
C_{22}	0.27	0.15	3.48	10.94	9.82	0.59	5.32	9.64	0.40	8.72	8.62	0.58	10.49
C_{23}	0.32	0.33	6.51	10.69	8.55	0.61	8.46	8.43	0.48	10.55	7.42	1.02	10.71
C_{24}	0.37	0.89	9.41	9.74	7.41	0.61	10.54	7.32	0.72	10.83	6.37	2.14	10.02
C_{25}	0.31	2.14	10.90	8.55	6.33	0.67	10.97	6.27	1.38	10.13	5.40	4.24	8.95
C_{26}	0.72	4.49	11.12	7.46	5.43	1.11	10.47	5.38	2.97	9.15	4.61	7.21	7.92
C_{27}	1.28	7.47	10.20	6.29	4.52	2.04	9.27	4.47	5.47	7.86	3.82	9.73	6.75
C_{28}	2.70	10.30	9.09	5.35	3.84	4.02	8.13	3.80	8.64	6.77	3.20	11.21	5.78
C_{29}	5.30	12.02	7.92	4.52	3.20	7.16	7.04	3.17	11.35	5.79	2.69	11.44	4.91
C_{30}	8.94	12.30	6.73	3.77	2.64	10.61	5.98	2.62	12.59	4.86	2.22	10.71	4.10
C_{31}	12.51	11.73	5.76	3.17	2.21	13.24	5.10	2.19	12.57	4.11	1.89	9.68	3.46
C_{32}	14.64	10.39	4.80	2.61	1.81	14.02	4.24	1.80	11.42	3.47	1.55	8.34	2.86
C_{33}	15.13	8.94	4.00	2.16	1.50	13.42	3.53	1.48	9.95	2.86	1.28	7.06	2.35
C_{34}	14.11	7.44	3.28	1.76	1.22	11.89	2.89	1.21	8.34	2.33	1.04	5.82	1.95
C_{35}	12.57	6.19	2.71	1.45	1.00	10.23	2.45	0.99	6.96	1.92	0.86	4.83	1.61
C_{36}	10.75	5.14	2.25	1.20	0.83	8.60	2.02	0.82	5.74	1.58	0.71	3.97	1.33

3. Calculation

As wax appearance is mainly caused by temperature decreases, pressure effects were neglected in most of wax precipitation models which are restricted to predict wax formation in low pressure systems [3] or stock tank oil [4–6], or synthetic mixtures under atmospheric pressure [7–9]. Nevertheless, as it has been seen in the experimental part, the influence of pressure on the formation of solid deposits is not insignificant. Thus, two models [10,11] were proposed to predict waxy solid deposits in condensate gas and live oil under high pressure. However, these models, which rests on the assumption that each heavy component crystallizes pure, are not in agreement with the works of Craig et al.

Table 3
Weight percentage of paraffins crystallized at the studied (P, T) conditions

P (MPa)			0.1				10			30			50
T (K)	290.2	283.5	273.2	263.7	256.2	290.2	273.2	256.2	290.2	273.2	256.2	290.2	273.2
Percentage of crystallization for each paraffin													
C_6	0.00	0.00	0.00	0.00	0.00	0.00	0.00	0.00	0.00	0.00	0.00	0.00	0.00
C_7	0.00	0.00	0.00	0.00	0.00	0.00	0.00	0.00	0.00	0.00	0.00	0.00	0.00
C_8	0.00	0.00	0.00	0.00	0.00	0.00	0.00	0.00	0.00	0.00	0.00	0.00	0.00
C9	0.00	0.00	0.00	0.00	0.00	0.00	0.00	0.00	0.00	0.00	0.00	0.00	0.00
C_{10}	0.00	0.00	0.00	0.00	0.00	0.00	0.00	0.00	0.00	0.00	0.00	0.00	0.00
C_{11}	0.00	0.00	0.00	0.00	0.00	0.00	0.00	0.00	0.00	0.00	0.00	0.00	0.00
C_{12}	0.00	0.00	0.00	0.00	0.00	0.00	0.00	0.00	0.00	0.00	0.00	0.00	0.00
C_{13}	0.00	0.00	0.00	0.00	0.28	0.00	0.00	0.00	0.00	0.00	0.33	0.00	0.00
C_{14}	0.00	0.00	0.00	0.00	1.09	0.00	0.00	0.00	0.00	0.00	1.58	0.00	0.00
C_{15}	0.00	0.00	0.00	0.00	1.19	0.00	0.00	0.00	0.00	0.00	3.25	0.00	0.28
C_{16}	0.00	0.00	0.00	0.66	3.20	0.00	0.00	3.16	0.00	0.04	11.02	0.39	0.29
C_{17}	0.00	0.00	0.00	1.34	10.77	0.00	0.00	14.41	0.00	0.08	30.45	0.42	0.74
C_{18}	0.00	0.00	0.00	4.16	29.12	0.00	0.00	37.04	0.00	0.67	55.52	0.71	2.75
C_{19}	0.00	0.00	0.10	12.53	53.97	0.15	0.64	61.21	0.50	2.94	73.32	0.87	9.14
C_{20}	0.00	0.00	1.01	29.85	73.16	0.31	2.85	76.73	0.61	9.80	83.02	1.07	23.83
C_{21}	0.03	0.09	3.95	51.98	83.80	0.43	9.24	85.17	0.75	24.52	88.40	1.36	44.84
C_{22}	0.09	0.22	11.79	69.95	89.43	0.59	22.84	90.18	1.01	44.90	91.92	2.21	63.58
C_{23}	0.13	0.59	26.28	80.89	92.77	0.73	42.00	93.42	1.43	63.16	94.24	4.65	75.74
C_{24}	0.18	1.89	44.73	86.95	95.11	0.87	59.92	95.65	2.54	75.47	95.78	11.11	82.89
C_{25}	0.18	5.41	61.33	90.74	96.76	1.14	72.50	97.25	5.75	83.12	96.77	24.21	87.43
C_{26}	0.50	13.29	73.47	93.35	97.88	2.24	80.38	98.21	13.95	87.94	97.39	42.73	90.72
C_{27}	1.08	26.36	81.41	95.28	98.61	4.91	85.37	98.82	28.37	91.16	97.83	60.59	93.21
C_{28}	2.73	42.46	86.60	96.77	100	11.35	88.94	100	46.84	93.59	98.14	73.91	95.14
C_{29}	6.49	57.95	90.13	97.82	100	23.11	91.69	100	63.87	95.42	98.40	82.62	96.52
C_{30}	13.52	70.49	92.75	98.69	100	38.91	93.85	100	76.28	96.82	98.60	88.18	97.49
C_{31}	23.20	79.28	94.77	99.09	100	54.27	95.45	100	83.96	97.80	100	91.56	98.17
C_{32}	34.01	84.75	96.18	99.46	100	66.22	96.46	100	88.37	100	100	93.65	98.66
C_{33}	43.59	87.94	97.12	99.64	100	73.94	97.12	100	90.74	100	100	94.77	98.37
C_{34}	50.81	89.61	97.67	99.74	100	78.58	97.62	100	92.00	100	100	95.32	100
C_{35}	55.59	90.32	97.92	100	100	81.10	100	100	92.55	100	100	95.61	100
C_{36}	58.00	90.92	98.71	100	100	82.17	100	100	92.60	100	100	95.51	100

[12] and Chevallier et al. [13–15] which found that petroleum waxes are made up of one or several solid solutions. Taking into consideration these structural observations a model, based on the assumption of a single orthorhombic waxy solid solution, has been proposed [1] to predict the wax appearance temperature as function of pressure in light gas–heavy hydrocarbons systems. This last model was used, in this work, to predict the wax content and the phases composition of the system studied.

The model rests on the Soave equation of state [16] modified with the volume translation introduced by Peneloux et al. [17] to represent the pressure influence on fluid phases (both liquid and vapor). However, as the mixture is composed of long and short chains components, the original quadratic classic mixing rule of the attractive term a is replaced by the LCVM mixing rule which has proved to lead to a satisfactory

representation of the vapor–liquid equilibrium of light–heavy asymmetric systems [18,19]. The excess Gibbs energy needed in this mixing rule is evaluated from the modified UNIFAC model [20].

According to the works of Craig et al. [12] and Chevallier et al. [13–15], the waxy solid phases are considered as solid solutions. The pressure effect on the fugacity of component i in the solid phase f_i^{S} is taken into account by means of the Poynting factor:

$$\ln \frac{f_i^{\mathrm{S}}(P)}{f_i^{\mathrm{S}}(P_0)} = \frac{1}{RT}\int_{P_0}^{P} \overline{V_i^{\mathrm{S}}}\,\mathrm{d}P \tag{6}$$

which is calculated by assuming that the partial molar volume in the solid phase $\overline{V_i^{\mathrm{S}}}$ is proportional to the molar volume in the liquid phase:

$$\overline{V_i^{\mathrm{S}}} = \bar{\beta} V_i^{\mathrm{L}}(x_i = 1) \tag{7}$$

where the coefficient $\bar{\beta}$ account for the excess volume in the solid phase and is evaluated to 0.90 from the structural measurements of Chevallier et al. [13]. With this assumption, the Poynting factor can be calculated using $\bar{\beta}$ and the fugacities of pure liquids. Thus, the fugacity of a paraffin i in the wax phase is evaluated by means of the following relation:

$$\ln f_i^{\mathrm{S}}(P) = \ln f_i^{\mathrm{S}}(P_0) + \overline{\beta} \ln \frac{f_i^{\mathrm{L}}(P, x_i = 1)}{f_i^{\mathrm{L}}(P_0, x_i = 1)} \tag{8}$$

where the atmospheric pressure fugacity of a component i in the solid phase is related to the pure solid fugacity by introducing an activity coefficient:

$$f_i^{\mathrm{S}}(P_0) = x_i^{\mathrm{S}} \gamma_i^{\mathrm{S}}(P_0) f_i^{\mathrm{S}}(P_0, x_i = 1) \tag{9}$$

The pure solid fugacity is determined by considering the difference of the Gibbs energy between the solid and the subcooled liquid at the temperature T. Thus, the fugacity of a component in the waxy solid phase becomes:

$$f_i^{\mathrm{S}}(P_0) = x_i^{\mathrm{S}} \gamma_i^{\mathrm{S}}(P_0) f_i^{\mathrm{L_0}}(P_0, x_i = 1) \exp\left(-\frac{\Delta_{\mathrm{SL}} H_i}{RT}\left(1 - \frac{T}{T_i^{\mathrm{SL}}}\right) - \frac{\Delta_{\mathrm{SS}} H_i}{RT}\left(1 - \frac{T}{T_i^{\mathrm{SS}}}\right)\right) \tag{10}$$

in which the enthalpy of fusion $\Delta_{\mathrm{SL}} H_i$ and solid–solid transitions $\Delta_{\mathrm{SS}} H_i$ as well the temperatures of transitions T_i^{SL}, T_i^{SS} are determined for both even and odd n-paraffins from a correlation of the values of Broadhurst [21] for the odd n-paraffins. The activity coefficient, which takes the non-ideality of the solid solution at atmospheric pressure into account, is determined through a Gibbs energy model. Hansen et al. [4] have considered waxes as ideal solutions whereas Won [3] and Pedersen et al. [5] has proposed to use the regular solution theory of Scatchard–Hildebrand in order to model the non-ideality of waxy solid phases. Nevertheless, in accordance with the results of comparative tests performed at atmospheric pressure [22] a predictive version of the Wilson equation [23] proposed by Coutinho et al. [24] has been considered. However, this equation which enables only a single solid solution is well adapted for wax appearance temperature calculation, but cannot predict solid phase splitting a few Kelvins below the cloud point [25]. To remedy this shortcoming an adaptation of the UNIQUAC model [26] to solid phases [27] has been considered here.

The interest of this liquid–solid calculation procedure comes from the fact that pressure effects and effects of the non-ideality of the solid solutions are uncoupled in the model. Non-ideality of solutions is

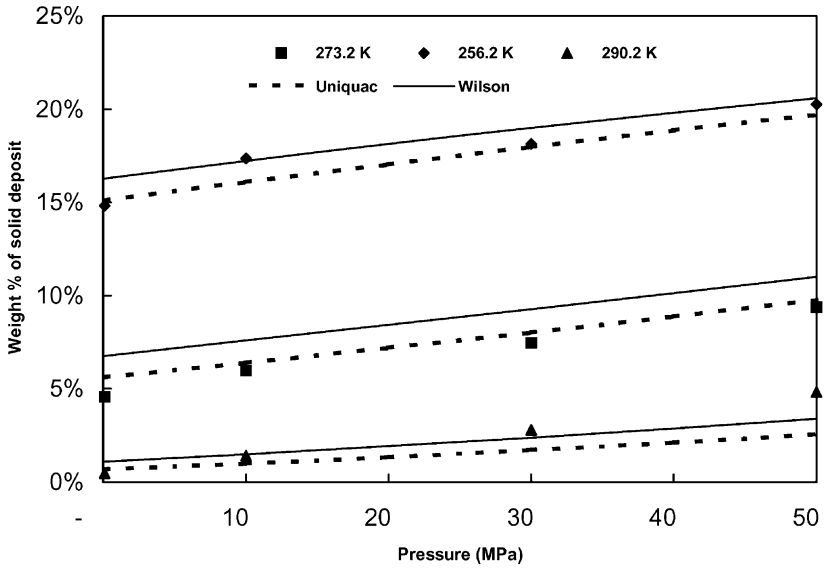

Fig. 4. Comparison of experimental and calculated solid deposit (in mass%) for three temperatures vs. pressure.

described through atmospheric Gibbs energy models while pressure effect is taken into consideration by means of the equation of state for the fluid phase.

4. Results and discussion

To compare the performance of the model using the Wilson equation or the UNIQUAC model, The predictions of the model without tuning any parameters were compared with the experimental data obtained for the mixture investigated. The quantity of solid deposit quantity as function of pressure was

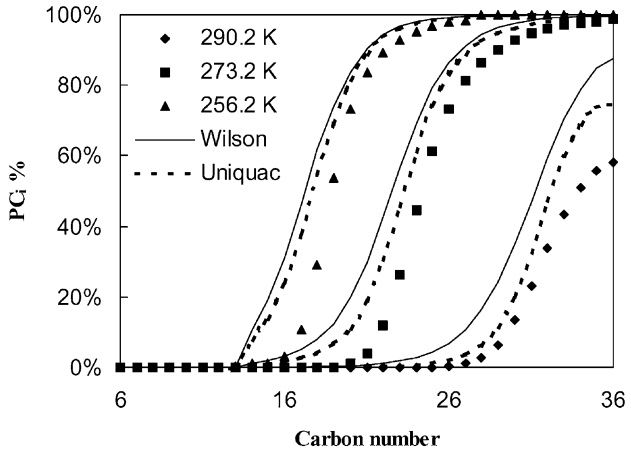

Fig. 5. Comparison of experimental and calculated weight percentage of crystallized paraffins for three temperatures at 0.1 MPa.

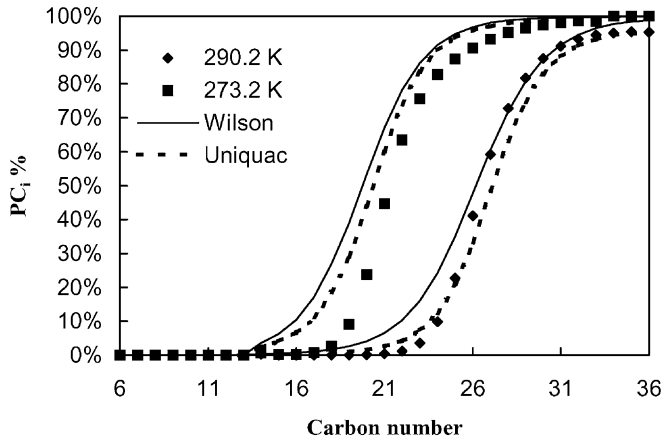

Fig. 6. Comparison of experimental and calculated weight percentage of crystallized paraffins for three temperatures at 50 MPa.

first used to test capacities of the model (Fig. 4). Both approaches (Wilson or UNIQUAC) provide a good estimation of the slope of the deposit line for all the studied temperatures, which means that the pressure dependence is well described by the model. This fact can be related to a good evaluation of the $\bar{\beta}$ parameter in the Poynting term. However, the use of Uniquac instead of Wilson equation leads to better agreement with experimental data. This tendency is also observed in Figs. 5 and 6 which present the percentage of crystallization as a function of carbon number of the components at different temperature at atmospheric pressure (Fig. 5) and 50 MPa (Fig. 6). It can be noted from these figures that UNIQUAC introduces a small shift of the curves along the abscissa, and thus, the calculated curves match the experimental points better. This means that the Wilson equation leads to an overestimation of the crystallization of intermediates paraffins whereas the UNIQUAC model seems to represent the crystallization of intermediate paraffins as well as of heaviest paraffins. This situation can be explained

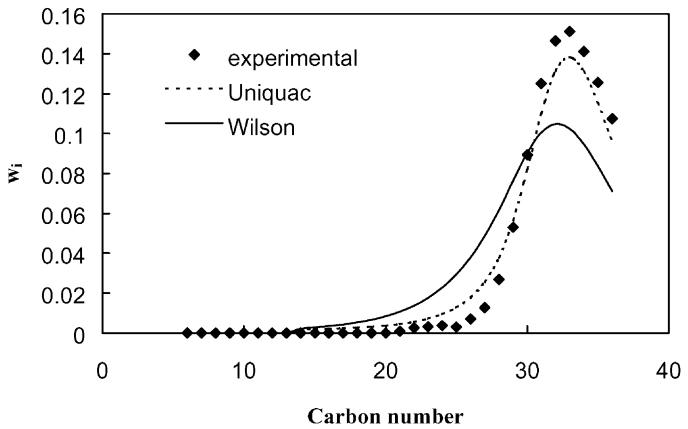

Fig. 7. Composition (in mass fraction) of the solid phase at 290.2 K and 0.1 MPa.

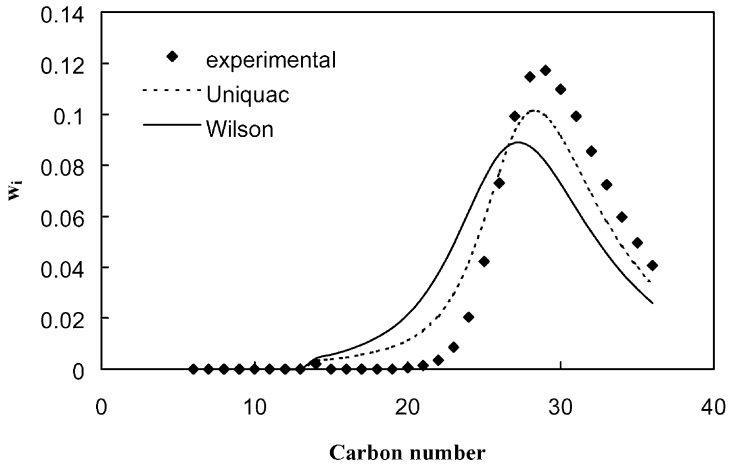

Fig. 8. Composition (in mass fraction) of the solid phase at 290.2 K and 50 MPa.

by the fact that when the Wilson equation is used the wax is assumed to be made up of a single solid solution of all the paraffins which may precipitate whereas with the UNIQUAC equation which allows solid–solid phase splitting the wax below the cloud point is composed essentially of heavies paraffins. Comparison of Figs. 5 and 6 shows that the model works equally well at atmospheric pressure and high pressure. This may suggest that the methodology employed to extrapolate the Gibbs excess model for the solid phase from atmospheric pressure to high pressure does not lead to major changes in the predictive capacity of the model.

The experimental data were also used to compare the effectiveness of the prediction of the wax composition (Figs. 7 and 8). It can be verified that the calculated curves are in good agreement with the experimental points. The shapes and the location of the maximum are well reproduced by the model. This result, which is achieved without any adjustments, shows that the model leads to a good description of the wax crystallization as a function of pressure. In particular, as it can be already observed at atmospheric pressure [28], solid phase splitting improves the representation of wax composition.

List of symbols

f	fugacity
H	enthalpy
L	liquid fraction (weight)
P	pressure
PC	wt.% of paraffins crystallized
R	ideal gas constant
S	solid fraction (weight)
T	temperature
V	volume
w	weight fraction
x	mole fraction

z feed composition in weight fraction
Z feed composition in mole fraction

Greek letters
α distribution composition
β volume change parameter
γ activity coefficient

Superscripts
L liquid
S solid
SL solid–liquid phase change
SS solid–solid phase transition
- partial properties

Subscripts
0 atmospheric
i component

Acknowledgements

The authors wish to thank the CNRS-ECODEV project on reservoir fluids for financial support of this research.

References

[1] J. Pauly, J.L. Daridon, J.A.P. Coutinho, N. Lindeloff, S.I. Andersen, Fluid Phase Equilibria 167 (2000) 145.
[2] J.L. Daridon, C. Dauphin, Meas. Sci. Tech. 10 (1999) 1309.
[3] K.W. Won, Fluid Phase Equilibria 30 (1986) 265.
[4] J.H. Hansen, Aa. Fredenslund, K.S. Pedersen, H.P. Ronningsen, AIChE J. 34 (1988) 1937.
[5] K.S. Pedersen, P. Skovborg, H.P. Ronningsen, Energy Fuels 5 (1991) 924.
[6] C. Lira-Galena, A. Firoozabadi, J.M. Prausnitz, AIChE 42 (1996) 239.
[7] K.W. Won, Fluid Phase Equilibria 53 (1989) 377.
[8] J.A.P. Coutinho, S.I. Andersen, E.H. Stenby, Fluid Phase Equilibria 103 (1995) 23.
[9] J.A.P. Coutinho, K. Knudsen, S.I. Andersen, E.H. Stenby, Chem. Eng. Sci. 51 (1996) 3273.
[10] P. Ungerer, B. Faissat, C. Leibovici, H. Zhou, E. Behar, Fluid Phase Equilibria 111 (1995) 287.
[11] H. Pan, A. Firoozabadi, P. Fotland, SPE Production and Facilities, November 1993, p. 250.
[12] S.R. Craig, G.P. Hastie, K.J. Roberts, A.R. Gerson, J.N. Sherwood, R.D. Tack, J. Mater. Chem. 8 (1998) 859.
[13] V. Chevallier, E. Provost, J.B. Bourdet, M. Bouroukba, D. Petitjean, M. Dirand, Polymer 40 (1999) 2121.
[14] V. Chevallier, D. Petitjean, M. Bouroukba, M. Dirand, Polymer 40 (1999) 2129.
[15] V. Chevallier, M. Bouroukba, D. Petitjean, M. Dirand, J. Pauly, J.L. Daridon, V. Ruffier-Meray, Fuel 79 (2000) 1743.
[16] G. Soave, Chem. Eng. Sci. 27 (1972) 1197.
[17] A. Peneloux, E. Rauzy, Fluid Phase Equilibria 8 (1982) 7.
[18] C.J. Boukouvalas, K.G. Magoulas, S.K. Stamataki, D.P. Tassios, Ind. Eng. Chem. Res. 36 (1997) 5454.
[19] N. Spiliotis, C.J. Boukouvalas, N. Tzouvaras, D.P. Tassios, Fluid Phase Equilibria 101 (1994) 187.
[20] J. Gmehling, Li Jidding, M. Schiller, Ind. Eng. Chem. Res. 32 (1993) 178.
[21] M.G. Broadhurst, J. Res. Nat. Bur. Stand. 66A (1962) 241–249.

[22] J. Pauly, C. Dauphin, J.L. Daridon, Fluid Phase Equilibria 149 (1998) 191.
[23] G.M. Wilson, J. Am. Chem. Soc. 86 (1964) 127.
[24] J.A.P. Coutinho, K. Knudsen, S.I. Andersen, E.H. Stenby, Ind. Eng. Chem. Res. 35 (1996) 918.
[25] V. Chevallier, A.J. Briard, D. Petitjean, N. Hubert, M. Bouroukba, M. Dirand, Mol. Cryst. Liq. Cryst., 2000, in press.
[26] D.S. Abrams, J.M. Prausnitz, AIChE J. 21 (1975) 116.
[27] J.A.P. Coutinho, Ind. Eng. Chem. Res. 37 (1998) 4870.
[28] C. Dauphin, J.L. Daridon, J. Coutinho, P. Baylère, M. Potin-Gautier, Fluid Phase Equilibria 161 (1999) 135.